Diagonal Walk Reference Generator based on Fourier Approximation of ZMP Trajectory

Rui Ferreira[4], Nima Shafii[124], Nuno Lau[34], Luis Paulo Reis[15], Abbas Abdolmaleki[134]

[1]Artificial Intelligence and Computer Science Laboratory (LIACC), University of Porto
[2] Dept. of Informatics Engineering, Faculty of Engineering of the University of Porto
[3]Dept. of Electronics, Telecommunications and Informatics, University of Aveiro
[4]Instituto de Engenharia Electronica e Telematica de Aveiro (IEETA) ,University of Aveiro
[5]School of Engineering, University of Minho
rui.ferreira@fe.up.pt, nima.shafii@fe.up.pt, nuno.lau@ua.pt,lpreis@fe.up.pt, abbas@ua.pt

Abstract— **Humanoid robots should be capable of adjusting their walking speed and walking direction. Due to the huge design space of the controller, it is very difficult to control the balance of humanoids walk. The position of the Zero Moment Point (ZMP) is widely used for dynamic stability measurement in biped locomotion. The reference trajectory of the Center of Mass (CoM) of a humanoid can be computed from a predefined ZMP trajectory. In order to generate the CoM trajectory, many researchers represent the ZMP equation using the motion equations of simple physical system, e.g. the cart-table model. A Fourier series approximation based method, which generates the CoM trajectory, was previously proposed for straight and curve walking. This paper extends these techniques to generate side and diagonal walking.**

In order to generate diagonal walking, straight and side walking are combined. The proposed CoM generation approach was tested on a simulated NAO robot. Experiments indicate that the method is successful in generating stable side and diagonal walking. Comparison results of the proposed method with ZMP preview control method show the benefits of the proposed technique.

Keywords— Biped Walking; Trajectory generation; diagonal walking;

I. Introduction

Humanoid robots are designed with high mobility capabilities. Wheeled locomotion is not appropriate for many human environments, such as stairs and areas littered by many obstacles. However, humanoid robots, due to a larger number of joints are able to avoid obstacles, and attain a wider variety of postures. Therefore, considering this advantage, humanoid robots can function and fulfill their tasks more easily than wheeled robots in domestic areas. In addition, due to the fact that biped locomotion is similar to human movement, people interact more easily with humanoid robots than with other types of robots.

Even though biped locomotion has advantages in many aspects, it is still not used in real common tasks, such as industrial and military activities. A humanoid robot contains many degrees of freedom which increase the dimension of the controller's design space. Due to the huge controller design space, as well as being an inherently nonlinear system, it is very difficult to control the balance of the humanoid robot during walking. The ZMP [1] criterion is widely used as a stability measurement in the literature. For a given set of walking trajectories, if the ZMP trajectory keeps firmly inside the area covered by the foot of the support leg or the polygon containing the support legs, the given biped locomotion will be physically feasible and the robot will not fall over during walking. Biped walking can be achieved by modelling the predefined ZMP references to the possible body swing or CoM trajectory. The possible CoM can be calculated by a simple model, approximating the bipedal robot dynamics, such as Cart-on-a-table or inverted pendulum model [2].

There is no straightforward way to compute CoM from ZMP by solving the differential equations of the cart-table model. The approaches presented previously, on how to tackle this issue, are organized into two major groups, optimal control approaches and analytical approaches. Kajita has presented an approach to find the proper CoM trajectory, based on the preview control of the ZMP reference, which makes the robot able to walk in any direction [3]. This is a dominant example of the optimal control approach. Some analytical approaches were also developed based on the Fourier series approximation technique, which can create straight walking reference [4] [5]. Recently this reference generation technique has been improved, and tested on the real humanoid robot to generate curve walking [6].

Although making a humanoid robot walk in a straight or curved line is very important and motivating for researchers, generating other types of walking such as side and diagonal walking can improve the ability of a humanoid robot to avoid obstacles. To the best of our knowledge, there is no method based on Fourier approximation to generate side and diagonal walking. Therefore, the contribution of this paper is to extend the Fourier based straight walking approach in [4] [5] into a side and diagonal walking generation approach. In order to create diagonal walking with desired speed, a combination of straight and side walking is required. The speeds on X and Y directions are varied according to user input, which allows the robot to change its walking direction. In order to test its performance, the proposed walking reference generation system is applied to the NAO simulated robot.

In this paper, the results are compared to another well-established method, the ZMP preview control approach. There are also no published studies which compare the outcome results of Fourier based approaches, with the results of the ZMP preview control approach. The experimental results outlined in this paper demonstrate that better side and diagonal walking can be achieved than has previously been achieved in the ZMP preview control approach. The reminder of paper is organized as follows. The next section outlines cart on the table model and how it can be used for humanoid walking. Section 3 explains the preview controller applied to the biped walking. The diagonal walking reference trajectory generation method based on Fourier approximation is described in Section 4. Experimental and comparison results are presented in Section 5. General conclusions and future work are discussed in the last section

II. CART-TABLE MODEL APPLIED ON THE BIPED WALKING

Many popular approaches used for joint trajectory planning for bipedal locomotion are based on ZMP stability indicator and cart-table model. ZMP cannot generate reference walking trajectories for walking directly but it can indicate whether generated walking trajectories will keep the balance of a robot or not. Nishiwaki proposed an approach to generate walking patterns by solving the ZMP equation numerically [7]. Kajita assumed that biped walking is a problem of balancing a cart-table model [2], since in the single supported phase, human walking can be represented as the Cart-table model or linear inverted pendulum model [3].

Biped walking can be modeled using the movement of ZMP and body swing. The robot is in balance when the position of the ZMP is in the support polygon. When the ZMP reaches to the edge of the polygon, the robot loses its balance. Biped walking can be achieved by modeling of the desired ZMP to the possible CoM. The body swing can be approximated by using dynamic model of a Cart-on-a-table.

Cart-table model has some assumptions and simplifications in its modeling. First, it assumes that all masses are concentrated on the cart. Second, it assumes that the support leg does not have any masses and represents itself as a massless table. Although these assumptions seem to be far from reality, modern walking robots usually have heavy bodies, with electronics circuits and batteries inside. Therefore the effect of leg mass is relatively small. Fig. 1 shows how robot dynamics is modeled by a cart on a table.

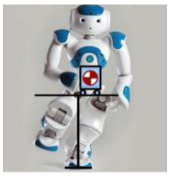

Fig. 1. Schematic view of Cart-table model and a humanoid robot

Two sets of cart-table are used for 3D walking. One is for movements in frontal plane; another is for movements in coronal plane. The semantic view of a cart-table is shown in fig. 2.

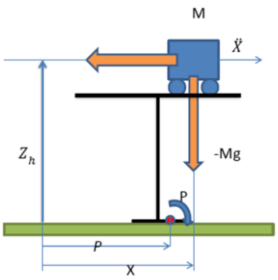

Fig. 2. Schematic view of Cart-table model and a humanoid robot

The position of Center of Mass M is x and Z_h defined in the coordinate system O. Gravity g and cart acceleration $\ddot{x}$ create a moment T_p around the center of pressure (CoP) point P_x. Equation (1) gives the sum of the torques at point P.

$$T_p = Mg(x - P_x) - M\ddot{x}z_h \tag{1}$$

We know from [8] that when the robot is dynamically balanced, ZMP and CoP is in the same point, therefore the amount of the moment in the CoP Point must be zero ,T_p=0. By Assuming the left hand side of equation (1) to be zero, equation (2) from position of the P_x and x can be derived. As mentioned before, to generate proper walking, the CoM must move in coronal plane and another cart-table must be used in y direction. Using the same assumption and reasoning, equation (3) can be obtained. Here, y index denotes the movement in y.

$$P_x = x - \frac{Z_h}{g}\ddot{x} \tag{2}$$

$$P_y = y - \frac{Z_h}{g}\ddot{y} \tag{3}$$

In order to apply cart-table model in a biped walking problem, first the position of the foot during walking must be planed and defined, then, based on the constraint of ZMP position and support polygon, the ZMP trajectory can be designed. In the next step, the position of the CoM from differential equations (2) (3) must be calculated. Finally, inverse kinematics is used to find the angular trajectories of each joint based on the planed position of the foot and calculated CoM.

The main issue of applying Cart-table Model is how to solve its differential equations. Even though theoretically CoM trajectory can be calculated by using the exact solution of the Cart-table differential equations, Applying calculated trajectory is not straightforward in a real biped robot walking because the solution consists of unbounded functions *cosh*, and the obtained CoM trajectory is very sensitive to the time step variation of the walking gait.

An alternative robust CoM trajectory generation method can be found in [4][5], in which the solution of the Cart-pole model differential equation is approximated based on Fourier representation of the ZMP equation. Kajita et. al [3] also presents a very applicable approach to calculate the position of the CoM from the cart-table model. This approach is based on the preview control of the ZMP reference which will be presented in the next section.

III. PREVIEW CONTROL APPROACH

In this section, the ZMP Preview Control Approach proposed by Kajita et al. will be explained [3], An extended explanation on its stability analysis is presented by Wieber [9]. The jerk $\dddot{x}$ of the cart areas of the system is assumed as input u of the cart table dynamics ($\dddot{x} = u$). Considering this assumption, the ZMP equation (2) can be converted to a strongly appropriate dynamical system which is presented in (4)

$$\frac{d}{dt}\begin{pmatrix} x \\ \dot{x} \\ \ddot{x} \end{pmatrix} = \begin{pmatrix} 0 & 1 & 0 \\ 0 & 0 & 1 \\ 0 & 0 & 0 \end{pmatrix}\begin{pmatrix} x \\ \dot{x} \\ \ddot{x} \end{pmatrix} + \begin{pmatrix} 0 \\ 0 \\ 1 \end{pmatrix} u \tag{4}$$

$$P = \begin{pmatrix} 1 & 0 & -\frac{Z_h}{g} \end{pmatrix}\begin{pmatrix} x \\ \dot{x} \\ \ddot{x} \end{pmatrix}$$

For the Cart table system, a digital controller is designed that allows the system output to follow the reference input. Digital controller input and error signal can be determined by equation (5).

$$u(k) = -G_i \sum_{i=0}^{k} e(i) - G_x x(k) \tag{5}$$

Here, G_i and G_x are assumed as the gain for the ZMP tracking error and the gain for state feedback respectively. x is the state of the system and denotes CoM positions, $x = [x\ \dot{x}\ \ddot{x}]^T$. k denoted the k^{th} sample time. Fig. 3 shows the block diagram of the system.

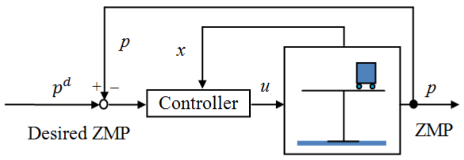

Fig. 3. ZMP Preview control Diagram

It was reported that the controller of equation (4) cannot follow the reference ZMP sufficiently. The main cause of this issue is the inherent phase delay. For addressing this problem, the original digital controller is redesigned in equation (6).

$$u(k) = -G_i \sum_{i=1}^{k} e(i) - G_x x(k) - \sum_{j=1}^{NL} G_p P^d(k+j) \tag{6}$$

The third term consists of the planed ZMP reference up to NL samples in future. The approach is called preview controller since the controller applies future information. The gain G_p is called the preview gain and its profile towards the future is shown in Fig. (4) The magnitude of the preview gain declines quickly with time. Therefore the ZMP preference can be neglected in the far future.

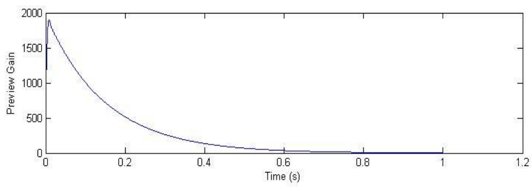

Fig. 4. Gain calculated based on the preview controller

IV. Fourier Series Approach

In this section the work in [4] is extended to endow the robot with a diagonal walk. First, the reference trajectory for the ZMP is formulated, and then it is approximated by using Fourier series. Finally, the position of the CoM is obtained by solving the differential equations (2) (3) of the cart-table dynamics while the source term P is assumed as the approximated ZMP.

In order to determine the reference trajectory of the ZMP, first the ZMP trajectory in a normal diagonal walk is analyzed. Fig. 5 shows the position of feet, on the ground plane, over t seconds.

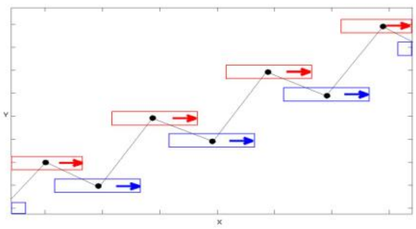

Fig. 5. Foot steps of a diagonal walking

To better understand the ZMP trajectory, ZMP movement is decomposed along X and Y axis, giving the advantage to illustrate them as functions of time. Figures (6) and (7) show the ZMP trajectories of X and Y, respectively.

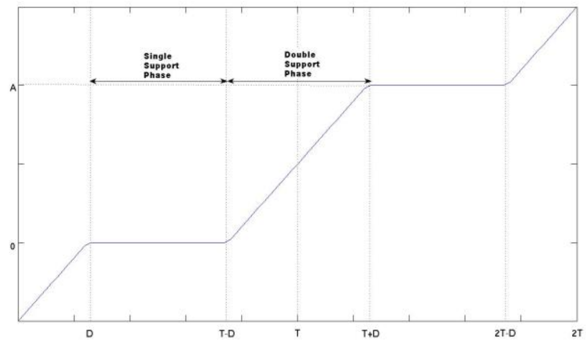

Fig. 6. ZMP trajectory in X direction

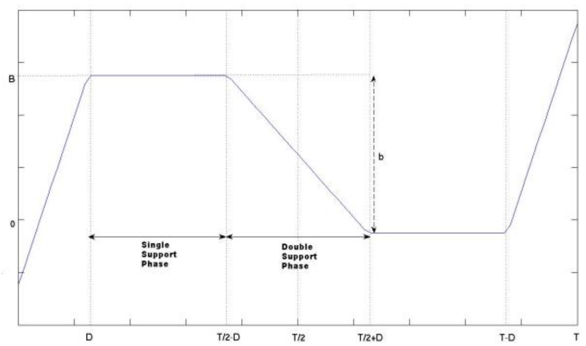

Fig. 7. ZMP trajectory in Y direction

ZMP trajectories can be seen as the combination of periodic and non-periodic component. Figures (8) and (9) illustrate the periodic and non-periodic components of the ZMP trajectories in the X and Y direction, respectively.

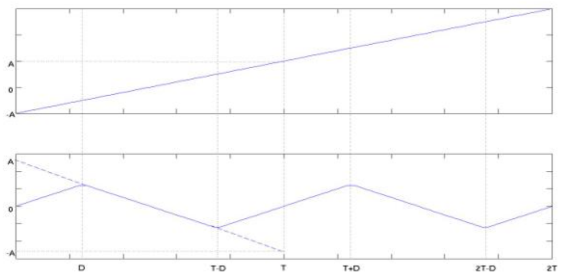

Fig. 8. ZMP component in X direction

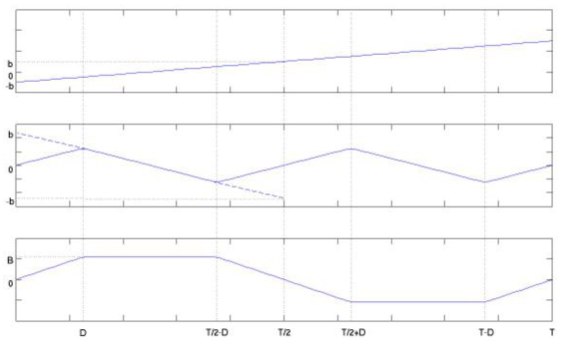

Fig. 9. ZMP component in Y direction

In order to employ Fourier series limited to a certain number of terms, continuous periodic functions are needed. Figures (8) and (9) are employed to determine the equations (7) and (12) for formulating the ZMP reference trajectory in X and Y direction respectively. The equations from (9) to (11) and from (14) to (23) formulate periodic components of the trajectory. The non-periodic component of the ZMP trajectories are presented in equations (8) (13).

This formulation design enhances the approach presented in [4] by adding a double support phase to formulate the ZMP trajectory, allowing to control the amount of double support phase using the parameter *D*. The parameters used in the ZMP trajectory formulation are listed in table (1) as well as a brief description of each one.

TABLE I. FORMULATION PARAMETERS

Parameter	Description
T	Period
A	Amount of displacement in X direction
B	Distance between both feet when walking straight
b	Amount of displacement in Y direction
D	Amount of time to be in double support phase

$$ZMP_x^{ref}(t) = f_{x1}(t) + \sum_{i=1}^{3} f_{2\_i}(t) \tag{7}$$

$$f_{x1}(t) = \frac{A}{T}\left(t - \frac{T}{2}\right) \tag{8}$$

$$f_{x2\_1}(t) = A\left(\frac{1}{2D} - \frac{1}{T}\right).t.\left(u(t) - u(t-D)\right) \tag{9}$$

$$f_{x2\_2}(t) = A\left(\frac{1}{2} - \frac{1}{T}\right)\left(u(t-D) - u(t-(T-D))\right) \tag{10}$$

$$f_{x2\_3}(t) = A\left(\frac{1}{2D} - \frac{1}{T}\right).(t-T).\left(u(t-(T-D)) - u(t-T)\right) \tag{11}$$

$$ZMP_y^{ref}(t) = f_y(t) + \sum_{i=1}^{5}\left(f_{y2\_i}(t) + f_{y3\_i}(t)\right) \tag{12}$$

$$f_{y1}(t) = \frac{b}{T}\left(t - \frac{T}{2}\right) \tag{13}$$

$$f_{y2\_1}(t) = \frac{2b\left(\frac{T}{4} - D\right)}{DT}.t.\left(u(t) - u(t-D)\right) \tag{14}$$

$$f_{y2\_2}(t) = -\frac{2b}{T}.\left(t - \frac{T}{4}\right).\left(u(t-D) - u\left(t - \left(\frac{T}{2} - D\right)\right)\right) \tag{15}$$

$$f_{y2\_3}(t) = \frac{2b\left(\frac{T}{4} - D\right)}{DT}.\left(t - \frac{T}{2}\right).\left(u\left(t - \left(\frac{T}{2} - D\right)\right) - u\left(t - \left(\frac{T}{2} + D\right)\right)\right) \tag{16}$$

$$f_{y2\_4}(t) = -\frac{2b}{T}.\left(t - \frac{3T}{4}\right).\left(u\left(t - \left(\frac{T}{2} + D\right)\right) - u\left(t - (T-D)\right)\right) \tag{17}$$

$$f_{y2\_5}(t) = \frac{2b\left(\frac{T}{4} - D\right)}{DT}.(t-T).\left(u(t-(T-D)) - u(t-T)\right) \tag{18}$$

$$f_{y3\_1}(t) = \frac{B}{D}.t.\left(u(t) - u(t-D)\right) \tag{19}$$

$$f_{y3\_2}(t) = B\left(u(t-D) - u\left(t - (\frac{T}{2} - D)\right)\right) \tag{20}$$

$$f_{y3\_3}(t) = -\frac{B}{D}.\left(t - \frac{T}{2}\right).\left(u\left(t - \left(\frac{T}{2} - D\right)\right) - u\left(t - \left(\frac{T}{2} + D\right)\right)\right) \tag{21}$$

$$f_{y3\_4}(t) = -B\left(u\left(t - \left(\frac{T}{2} + D\right)\right) - u\left(t - (T-D)\right)\right) \tag{22}$$

$$f_{y3\_5}(t) = \frac{B}{D}.(t-T).\left(u(t-(T-D)) - u(t-T)\right) \tag{23}$$

The next step is to determine the Fourier series of equations (7) and (12). For this we used the definition of the Fourier series given by (24).

$$f(t) = \frac{a_0}{2} + \sum_{n=1}^{N}\left[a_n\cos(nt) + b_n\sin(nt)\right],\ N \geq 1 \tag{24}$$

The results are given by equations (25) and (26) which are approximated ZMP trajectories using Fourier series definition (24).

$$ZMP_x^{fourier}(t) = \frac{A}{T}\left(t - \frac{T}{2}\right) + \sum_{n=1}^{N}\left[b_{n\_x}\sin\left(\frac{2n\pi}{T}t\right)\right], N \geq 1 \tag{25}$$

$$ZMP_y^{fourier}(t) = \frac{b}{T}\left(t - \frac{T}{2}\right) + \sum_{n=1}^{N}\left[b_{n\_y}\, sin\left(\frac{2n\pi}{T}t\right)\right], N \geq 1 \quad (26)$$

Where

$$b_{n\_x} = \left(\frac{2A\sin\left(\frac{2n\pi}{T}\times DSP\right)}{T.DSP.\left(\frac{2n\pi}{T}\right)^2}\right) \quad (27)$$

$$b_{n\_y} = \left(\frac{2\,sin\left(\frac{2n\pi}{T}\times DSP\right)}{T.DSP.\left(\frac{2n\pi}{T}\right)^2}\right)\left((b-B)(-1)^2 + B + b\right) \quad (28)$$

Finally, it remains to solve the cart-table differential equations (2) and (3) using equations (25) and (26) as source term.

$$y - \frac{Z_h}{g}\ddot{y} = \sum_{n=1}^{N}\left[b_n\, sin\left(\frac{2n\pi}{T}t\right)\right], \quad N \geq 1 \quad (29)$$

The value of the parameter *N* must be a positive integer. The solution will be of the form:

$$y(t) = \sum_{n=1}^{N}\left[C_n \sin\left(\frac{2n\pi}{T}t\right)\right] \quad (30)$$

$$\ddot{y}(t) = \sum_{n=1}^{N}\left[-C_n\left(\frac{2n\pi}{T}\right)^2 sin\left(\frac{2n\pi}{T}t\right)\right] \quad (31)$$

By substituting equations (30) and (31) to (29), the (32) is obtained.

$$\sum_{n=1}^{N}\left[C_n \sin\left(\frac{2n\pi}{T}t\right)\right] - \frac{Z_h}{g}\sum_{n=1}^{N}\left[-C_n\left(\frac{2n\pi}{T}\right)^2 sin\left(\frac{2n\pi}{T}t\right)\right] = \sum_{n=1}^{N}\left[b_n \sin\left(\frac{2n\pi}{T}t\right)\right] \quad (32)$$

This equality is true when:

$$C_n - \frac{Z_h}{g}\left(-C_n\left(\frac{2n\pi}{T}\right)^2\right) = b_n \quad (33)$$

Solving for C_n and substituting to (30) we get the particular solution for the second order differential equation:

$$y(t) = \sum_{n=1}^{N}\left[\left(\frac{b_n}{\left(1 + \frac{Z_h}{g}\left(\frac{2n\pi}{T}\right)^2\right)}\right)\sin\left(\frac{2n\pi}{T}t\right)\right] \quad (34)$$

To get the CoM equation all we have to do is to solve the differential equation (29) but changing the right side of the equation with the corresponding ZMP equations (25) and (26). The results are given by equations (35) and (36).

$$CoM_x(t) = \frac{A}{T}\left(t - \frac{T}{2}\right) + \sum_{n=1}^{N}\left[\left(\frac{b_{n\_x}}{\left(1 + \frac{Z_h}{g}\left(\frac{2n\pi}{T}\right)^2\right)}\right)\sin\left(\frac{2n\pi}{T}t\right)\right] \quad (35)$$

$$CoM_y(t) = \frac{b}{T}\left(t - \frac{T}{2}\right) + \sum_{n=1}^{N}\left[\left(\frac{b_{n\_y}}{\left(1 + \frac{Z_h}{g}\left(\frac{2n\pi}{T}\right)^2\right)}\right)\sin\left(\frac{2n\pi}{T}t\right)\right] \quad (36)$$

V. RESULTS AND DISCUSSIONS

According to section 2, the CoM reference trajectory is obtained by solving the Cart-Table model. Position trajectories of the swing foot are generated through Bézier curve based on predefined footsteps. The swing foot orientation is kept parallel to the ground to reduce the effect of the contact force. Joint angles are calculated based on swing foot positions and CoM references by using inverse kinematics, then joints are controlled by simple independent PID position controllers. The detailed explanation of the techniques, used for inverse kinematics and control of the swing foot positions, can be found in [10] [11].

In this study, a simulated NAO robot is used in order to test and verify the approach. The NAO model is a kid size humanoid robot which has 58 cm height and 21 degree of freedom (DoF). The link dimensions of the NAO robot can be found in [12]. The simulation is carried out by RoboCup soccer simulator, rcsssever3d, which is the official simulator released by the RoboCup community, in order to simulate humanoids soccer match. The simulator is based on Open Dynamic Engine and Simspark [13].

According to literature, there are no published studies to compare the performance of the Fourier based ZMP approximation approach and ZMP preview control approach. In order to test and compare the performance of aforementioned approaches, several robot walking scenarios were designed, in which the simulated NAO robot walks with different speeds from 0 to 0.6 m/s in different directions. The scenarios are designed for different speeds with 0.15 m/s increment in X and Y direction, while the overall speed should not exceed the maximum speed. Parameters used in the walking scenarios are presented in Table 2.

TABLE II. PARAMETERS OF WALKING SCENARIO

Parameters	Value
Step Period	0.2 s
Step Height of the swing foot	0.02 m
Step Size in X direction	3 ,6, 9 ,12 cm
Step Size in Y direction	3, 6, 9 ,12 cm
Percentage of the Double Support Phase (DSP) to the whole step time	15 %
Time of whole walking	4 s, 20 steps
Height of the inverted pendulum (Z_h)	0.22 cm

All walking scenarios are simulated in the same machine with the same specification. Mean Absolute Error (MAE) of the predefined reference ZMP trajectory and computed ZMP using the two approaches are presented in table 3. The number of the Fourier terms denoted by *N* is assumed to be 8. The incremental times of the preview control loop denoted by *dt* are assumed to be 0.01, 0.001 and 0.0001.

TABLE III. MAE OF COMPUTED ZMP AND REFERENCE ZMP TRAJECORY

Speed	**Mean Absolute Error (MAE in X direction, MAE in Y direction)**			
(Speed$_X$, Speed$_Y$)	***Fourier , N=8***	***Preview , dt=0.01***	***Preview , dt=0.001***	***Preview, dt=0.0001***
(0.15,0)	(0.0001167,0.0018)	(0.0044,0.0061)	(0.0031,0.0025)	(0.0022,0.0014)
(0.3 ,0)	(0.0002335,0.0018)	(0.0091,0.0061)	(0.0058,0.0025)	(0.0047,0.0014)
(0.45,0)	(0.0003503,0.0018)	(0.0137,0.0061)	(0.0087,0.0025)	(0.0070,0.0014)
(0.6 ,0)	(0.0004671,0.0018)	(0.0183,0.0061)	(0.0116,0.0025)	(0.0093,0.0014)
(0, 0.15)	(0, 0.0018)	(0 ,0.0089)	(0,0.0045)	(0,0.0031)
(0.15, 0.15)	(0.0001167,0.0018)	(0.0046 ,0.0089)	(0.0029,0.0045)	(0.0023,0.0031)
(0.3 , 0.15)	(0.0002335,0.0018)	(0.0091,0.0089)	(0.0058,0.0045)	(0.0047,0.0031)
(0.45, 0.15)	(0.0003503,0.0018)	(0.0137 ,0.0089)	(0.0087,0.0045)	(0.0070,0.0031)
(0 , 0.3)	(0, 0.0018)	(0, 0.0117)	(0, 0.0065)	(0, 0.0049)
(0.15 , 0.3)	(0.0001167,0.0018)	(0.0046, 0.0117)	(0.0029, 0.0065)	(0.0023, 0.0049)
(0 .3 , 0.3)	(0.0002335,0.0018)	(0.0091, 0.0117)	(0.0058, 0.0065)	(0.0047, 0.0049)
(0, 0.45)	(0 , 0.0019)	(0 , 0.0145)	(0 , 0.0085)	(0 , 0.0066)
(0.15, 0.45)	(0.0001167,0.0019)	(0.0046 , 0.0145)	(0.029, 0.0085)	(0.0023 , 0.0066)
(0, 0.6)	(0 , 0.0020)	(0 , 0.0174)	(0 , 0.00105)	(0 , 0.0083)

In average, The MAE in X and Y direction are achieved by the proposed Fourier method are 25 and 3 times less, respectively, than achieved by the preview control approach. Although by decreasing *dt*, the MAE of the preview control will be decreased, but achieving to the performance of the Fourier approach, practically, is not possible. Since the execution time of the algorithm will be increased dramatically. The average and variation of execution times for different specifications on the preview control and Fourier approach are presented in the table 4.

TABLE IV. THE AVERAGE (VAR) EXECUTION TIMES OF THE METHODS

Fourier , *N*=8	**Preview , *dt*=0.01**	**Preview , *dt*=0.001**	**Preview , *dt*=0.0001**
0.0458(1.8482e-006)	0.3013(5.9957e-005)	0.6306(0.0015)	16.5349(0.0014)

After executing the methods for each walking scenarios on the machine, the average execution times for approximating ZMP and generating CoM trajectories, by using the Fourier based approach, was 0.0458 second. It is 15 times faster than the best computation time that could be achieved by using the preview control approach. For a humanoid robot that has limited computational resources, performing a real time task, such as controlling the walking, requires an algorithm with low time complexity like Fourier based approach.

CoM reference and CoM position projection on the ground plane for the walking scenario, which has 15 cm/s speed in X direction and 15 cm/s in Y direction, are shown in fig. 10. The generated reference CoM trajectory and executed CoM trajectory by the robot are shown in blue and red lines respectively.

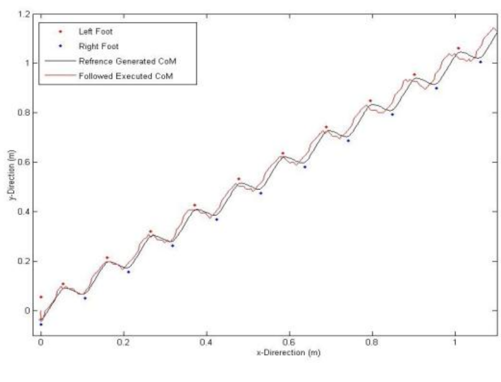

Fig. 10. COM (lines) for the diagonal walk

VI. CONCLUSIONS AND FUTURE WORK

In this paper an approach to generate the CoM reference trajectory of a diagonal and side walking is proposed. It is the first time that, by using the Fourier approximation on the predefine ZMP reference, CoM trajectories of diagonal and side walking is achieved. In order to test and validate the results, walking scenarios for the simulated NAO robot with different speeds are presented. The comparison results show that the accuracy and time computation complexity of the proposed method is better compared to the preview control approach.

In future work, the proposed method will be tested and implemented on a real humanoid robot. Our aim will be creating an omni-directional walking. Although the experimental results show that the robot can perform forward, side and diagonal walking successfully, extending the approach to make the robot able to do turn in place or curved walking, is also needed, to have a proper omni-directional walking.

REFERENCES

[1] M. Vukobratović and D. Juricić, “Contribution to the synthesis of biped gait.,” *IEEE Transactions on Biomedical Engineering*, vol. 16, no. 1, pp. 1–6, 1969.

[2] S. Kajita, F. Kanehiro, K. Kaneko, K. Yokoi, and H. Hirukawa, “The 3D linear inverted pendulum mode: a simple modeling for a biped walking pattern generation,” in *IEEE/RSJ International Conference on Intelligent Robots and Systems*, 2001, pp. 239–246.

[3] S. Kajita, F. Kanehiro, K. Kaneko, and K. Fujiwara, “Biped walking pattern generation by using preview control of zero-moment point,” in *IEEE International Conference on Robotics and Automation ,ICRA 2003*, 2003, pp. 1620–1626.

[4] K. Erbatur and O. Kurt, “Natural ZMP Trajectories for Biped Robot Reference Generation,” *IEEE Transactions on Industrial Electronics*, vol. 56, no. 3, pp. 835–845, Mar. 2009.

[5] Y. Choi, B. J. You, and S. R. Oh, “On the stability of indirect ZMP controller for biped robot systems,” in *2004 IEEE/RSJ International Conference on Intelligent Robots and Systems (IROS)*, 2004, pp. 1966–1971.

[6] M. Yilmaz, U. Seven, K. C. Fidan, T. Akbas, and K. Erbatur, “Circular arc-shaped walking trajectory generation for bipedal humanoid robots,” in *12th IEEE International Workshop onAdvanced Motion Control (AMC)*, 2012, pp. 1–8.

[7] K. Nishiwaki, S. Kagami, Y. Kuniyoshi, M. Inaba, and H. Inoue, “Online generation of humanoid walking motion based on a fast generation method of motion pattern that follows desired ZMP,” in *IEEE/RSJ International Conference on Intelligent Robots and System*, 2002, pp. 2684–2689.

[8] A. Goswami, “Postural Stability of Biped Robots and the Foot-Rotation Indicator (FRI) Point,” *The International Journal of Robotics Research*, vol. 18, no. 6, pp. 523–533, Jun. 1999.

[9] P. Wieber, “Trajectory Free Linear Model Predictive Control for Stable Walking in the Presence of Strong Perturbations,” in *2006 6th IEEE-RAS International Conference on Humanoid Robots*, 2006, pp. 137–142.

[10] R. Ferreira, L.P. Reis, A. P. Moreira, N. Lau, "Development of an Omnidirectional Kick For a NAO Humanoid Robot", *13th Ibero-American Conference on AI , LNAI* 7637, pp 571-580 ,2012.

[11] E. Domingues, N. Lau, B. Pimentel, N. Shafii, L. P. Reis, A. J. R. Neves, "Humanoid Behaviors: From Simulation to a Real Robot", *15th Portuguese Conference on Artificial Intelligence, EPIA 2011, LNAI 7367*, pp 352-364, 2011.

[12] D. Gouaillier, V. Hugel, P. Blazevic, C. Kilner, J. Monceaux, P. Lafourcade, B. Marnier, J. Serre, and B. Maisonnier, “Mechatronic design of NAO humanoid,” in *Proceedings of the IEEE International Conference on Robotics and Automation (2009)*, 2009, pp. 769–774.

[13] J. Boedecker and M. Asada, “SimSpark – Concepts and Application in the RoboCup 3D Soccer Simulation League,” *Autonomous Robots*, pp. 174–181, 2008.